Regularized Inversion of the Laplace Transform for Series of Experiments

B. Radel [†], E. H. Hardy,
Z. Djuric[‡], M. Mahlbacher[‡], M. Haist[‡], H. S. Müller[‡]

November 2018

Abstract: *Not only in Low-Field NMR, Laplace inversion is a relevant and challenging topic. Considerable conceptual and technical progress has been made, especially for the inversion of data encoding two decay dimensions. Distortion of spectra by overfitting of even moderate noise is counteracted requiring a priori smooth spectra. In this contribution, we treat the case of simple and fast one-dimensional decay experiments which are repeated many times in a series in order to study the evolution of a sample or process. Incorporating the a priori knowledge that also in the series dimension evolution should be smooth, peak position can be stabilized and resolution improved in the decay dimension. It is explained how the standard one-dimensional regularized Laplace inversion can be extended quite simply in order to include regularization in the series dimension. Obvious improvements compared to series of one-dimensional inversions are presented for simulated as well as experimental data. For the latter, comparison with multi-exponential fitting is performed.*

1 Introduction

Especially in Low Field NMR information on the sample is sought-after by the analysis of signal decays [1, 2]. If the signal is known beforehand to consist of one, two or maybe three mono-exponential contributions, the weights as well as decay times can be obtained by a corresponding least squares fit. If a distribution of relaxation rates exists, the ideal signal is the Laplace transform of the distribution of interest. Whereas regaining a distribution or spectrum of oscillation frequencies by discrete inverse Fourier transform is well-established, the inverse Laplace transform is challenging. Obtaining numerically a discrete positive distribution that minimizes the squared norm of the residuals between the predicted and observed signal works reliably. However, already for mildly different measured or simulated noise, quite

Institute of Mechanical Process Engineering and Mechanics, Karlsruhe Institute of Technology
[†]Corresponding author: benjamin.radel@kit.edu
[‡]Institute of Concrete Structures and Building Materials, Karlsruhe Institute of Technology

DOI: 10.1002/mrc.4836

different distributions are obtained. The Laplace inversion can be stabilized by adding a suitable cost function to the squared residuals in the minimization process. The cost function favors distributions which are smooth, which is a priori expected to be realistic [3]. Weighting the cost function with a regularization parameter allows for a trade-off between excessive smoothing and over-fitting. It can be chosen e.g. by the L-curve method [4, 5]. More advanced methods yield improved inversion results for distributions that are not necessarily smooth [6–10].

Laplace inversion has been extended to recover two-dimensional decay distributions, e.g. T_1-T_2 or diffusion-T_2 [11–14]. Measured data and the discrete distribution can be organized as one vector, respectively, and the matrix describing the Laplace transform is extended correspondingly by an operation referred to as Kronecker product. For the large matrix, data can be reduced by singular-value decomposition (SVD) and limitation to the biggest singular values. This is still an active field of research, see e.g. [15–19] and literature cited therein. Regularization can be adapted locally [15], methods making use of two regularization parameters may be used [16], combinations with parallel particle swarm optimization algorithms have been applied [17], 2D delta-like distributions were utilized [18] and inversion without Kronecker product was reported [19].

In this contribution, we demonstrate how Laplace inversion can be improved in applications, where a simple and fast one-dimensional decay experiment, e.g. CPMG, is repeated in a series consisting of many experiments, in order to study the evolution of the sample. Series occur e.g. if reactions such as resin curing are monitored by CPMG measurements of transverse signal decay [20]. Similar measurements have been conducted to study the hydration of cement paste [21]. Measuring transverse signal decay for series of temperatures and applying Laplace inversion is also of interest in cryoporometry, as explained in [22]. Acquisition of longitudinal signal decay for a series of polarizing fields are performed in field-cycling experiments, see e.g. [23]. In order to study restricted diffusion, PGSE diffusion signal decay can be acquired for a series of diffusion timescales, as explained in [24]. If diffusion signal decay is acquired with chemical-shift spectral resolution, the spectral dimension can be considered as series dimension [6, 7, 25]. In all of these cases, the data set is 2D, but in the second dimension the evolution is observed, in contrast to 2D experiments where two properties of the sample are spread and thus better resolved in two dimensions.

In the special case of a series of measurements where the sample is not expected to change its properties, a series of relaxation spectra without changes in series dimension is expected after inversion in decay dimension. Now this can be enforced by using one spectrum for the simultaneous description of all measurements in the series. Technically, this can be implemented by organizing all measurements in one vector and column-wise repetition of the matrix of the discrete Laplace transform. In simulations with different random noise per repetition, better distributions were recovered using the a priori knowledge of identical spectra compared to Laplace inversion of the averaged data or averaging the individual Laplace inversions.

In the general case of a sample with properties evolving during the series, we suggest adding a cost function favoring also a smooth evolution in the series dimension. As peaks in the

DOI: 10.1002/mrc.4836

relaxation spectrum may appear and disappear, at least in series dimension smoothing using the discrete second derivative rather than the identity matrix is advisable, as it is also recommended for two decay dimensions [15]. Technically, measured data can be vectorized as in the special case of no evolution, but now the Kronecker product of the identity matrix with the Laplace transform matrix yields as many spectra as experiments in the series. The matrices implementing the cost functions in decay and series dimension are weighted by two different regularization parameters. The resulting large amount of data is reduced using SVD. In [13], the more complex case of series of 2-D decay experiments, termed as 2.5-D experiment, is treated using the identity matrix for regularization of the series. This is equivalent to a separate 2-D Laplace inversion for each experiment in the series, however, the same regularization parameter is chosen for the entire series. Regularization of series of 2-D decay experiments with second-derivative regularization in series dimension would be more complex.

As a further improvement in view of a quantitative analysis of the series of spectra, the cumulative sum of the spectra rather than the spectra are used for smoothing in series dimension. Frequently, quantitative analysis is based on integration of spectral regions, as it is the case for the calculation of quantiles. Spectral contributions at decay times close to the dead time have only little influence on the predicted signal but a constant influence on the integrated spectrum, including the overall integral. As constraint in the optimization, the cumulative spectra have to be monotonically increasing, corresponding to non-negative spectra.

After a more specific description of the methods and their implementation, the benefits of second-derivative regularization of cumulative spectra in series dimension is first demonstrated on simulated experimental data. Next, a series of experimental CPMG decay data measured during a Furfuryl alcohol polymerization are inverted with regularization in series dimension and for comparison with standard regularization. Finally, CPMG decay data of a hydration experiment are inverted and compared to tri-exponential fitting. The evolution of the time constants and corresponding weights can be compared with the results of the inversion.

2 Methods

2.1 Laplace Inversion

The vector $\vec{y} \in \mathbb{R}^{n_T}$ collecting $n_T \in \mathbb{N}$ digitized measurement data y_i at times t_i can be written as

$$\vec{y} = \boldsymbol{A} \cdot \vec{g} + \vec{r}$$

with the Laplace transformation matrix $\boldsymbol{A} \in \mathbb{R}^{n_T \times n_S}$, the vector $\vec{g} \in \mathbb{R}_{>0}^{n_S}$ containing $n_S \in \mathbb{N}$ weights g_j for previously chosen decay times $s_j \in \mathbb{R}_{>0}$ and the vector $\vec{r} \in \mathbb{R}^{n_T}$ holding the

DOI: 10.1002/mrc.4836

residues. The matrix $\boldsymbol{A}$ represents the discrete Laplace transformation and is defined as

$$\boldsymbol{A} = \left(A_{ij}\right) = \left(\exp\left(-\frac{t_i}{s_j}\right)\right) \in \mathbb{R}^{n_T \times n_S},$$

with n_T as the number of measurement points and n_S as the number of predefined decay times. Obviously, the decay times s_j have to be chosen with regard to the expected real decay times of the components in the sample. Since the Laplace inversion is ill-defined, the singular values of matrix $\boldsymbol{A}$ decay quickly towards zero. Hence, a method is to be found that reduces the amount of data and increases the calculation speed. Therefore, the matrix $\boldsymbol{A}$ is compressed using SVD:

$$\boldsymbol{A} = \boldsymbol{U} \cdot \boldsymbol{\Sigma} \cdot \boldsymbol{V}^T.$$

The matrix $\boldsymbol{A}$ is split into three matrices $\boldsymbol{U} \in \mathbb{R}^{n_T \times n_T}$, $\boldsymbol{\Sigma} \in \mathbb{R}^{n_T \times n_S}$ and $\boldsymbol{V} \in \mathbb{R}^{n_S \times n_S}$, where $\boldsymbol{\Sigma}$ is a diagonal matrix padded with zeros containing the singular values in decreasing order and the matrices $\boldsymbol{U}$ and $\boldsymbol{V}$ are orthogonal. In this study only the 30 largest singular values are considered. The remaining singular values are neglected. Since the necessary amount of singular values is dependent on the decay times and the sample times, the number of singular values has to be adjusted for each purpose carefully. In our study, the number of singular values was chosen such that the ratio of the largest to the smallest considered singular value is at least 1×10^9 for all evaluated experiments. Using the SVD the compressed data (indicated with the hat symbol) equals to

$$\hat{\vec{y}} = \hat{\boldsymbol{U}}^T \cdot \vec{y} = \hat{\boldsymbol{\Sigma}} \cdot \hat{\boldsymbol{V}}^T \cdot \vec{g} + \hat{\boldsymbol{U}}^T \cdot \vec{r} = \hat{\boldsymbol{A}} \cdot \vec{g} + \hat{\vec{r}}$$

and yields to a compressed transformation matrix $\hat{\boldsymbol{A}} \in \mathbb{R}^{30 \times n_S}$. To find the weights $\vec{g}$ for the given decay times s_j the residuals $||\hat{\vec{y}} - \hat{\boldsymbol{A}} \cdot \vec{g}||_2^2$ are minimized via an optimization algorithm. Since this optimization problem is ill-posed, the obtained the results are highly influenced by the noise in the measured data. To compensate over-fitting, regularization is used to incorporate a priori knowledge of the expected results. A reasonable assumption is to require the weights' spectrum to be smooth. This is achieved by adding penalty functions to the optimization problem, which lead to a reduction of the second derivative and hence to a smoother spectrum. The degree of regularization can be adjusted by the regularization parameter. To find a proper regularization parameter the L-curve method according to [4] is used. The cost function of the regularization plotted versus the squared residuals for various regularization parameters leads to an L-shaped curve. In the maximum curvature of this curve a good trade off between regularization and signal fitting is achieved.

When applied to noisy signals, this method still provides unsatisfactory spectra. In this study the authors hence introduce a new regularization method which is applicable to measurement series. Such series could be a time-resolved reaction or a drying experiment. In such cases the peaks in the decay spectra are assumed not to spontaneously appear or disappear, but shift and de- or increase. Hence, a regularization in the dimension of measurement series is introduced to improve the overall Laplace inversion.

DOI: 10.1002/mrc.4836

Therefore, the $n_E \in \mathbb{N}$ vectors $\vec{y}_k$ containing the single measurements are concatenated to a vector $\vec{y}_l \in \mathbb{R}^{n_T n_E}$ containing all measurements:

$$\vec{y}_l = \begin{pmatrix} \vec{y}_1^T & \vec{y}_2^T & \cdots & \vec{y}_{n_E}^T \end{pmatrix}^T \in \mathbb{R}^{n_E n_T}$$

Now the Laplace inversion matrix needs to be adjusted. The matrix $\hat{\boldsymbol{A}}_{\boldsymbol{l}} \in \mathbb{R}^{30n_E \times n_E n_S}$ for the elongated measurement vector can be constructed by using the Kronecker product of the Identity matrix $\boldsymbol{I}_{\boldsymbol{l}} \in \mathbb{R}^{n_S \times n_S}$ and the compressed Laplace transformation matrix for a single dataset $\hat{\boldsymbol{A}}$:

$$\hat{\vec{y}}_l = \hat{\boldsymbol{A}}_{\boldsymbol{l}} \cdot \vec{g}_l + \hat{\vec{r}}_l = \boldsymbol{I}_{\boldsymbol{l}} \otimes \hat{\boldsymbol{A}} \cdot \vec{g}_l + \hat{\vec{r}}_l$$

with $\vec{g}_l \in \mathbb{R}^{n_E n_S}$ and $\hat{\vec{r}}_l \in \mathbb{R}^{30n_E}$. Obviously, the resulting weights vector is also concatenated and holds all resulting spectra in one vector when performing the Laplace inversion.

The regularization matrices are now added in the same way to the optimization problem. In the resulting equation

$$\vec{d} = \begin{pmatrix} \hat{\vec{y}}_l^T & \vec{0}^T & \vec{0}^T \end{pmatrix}^T = \begin{pmatrix} \hat{\boldsymbol{A}}_{\boldsymbol{l}}{}^T & \alpha \boldsymbol{D}^T & \gamma \boldsymbol{C}^T \end{pmatrix}^T \cdot \vec{g}_l + \begin{pmatrix} \hat{\vec{r}}_l^T & \vec{0}^T & \vec{0}^T \end{pmatrix}^T$$

two additional matrices are introduced. The product of matrix $\boldsymbol{D} \in \mathbb{R}^{(n_S-2)n_E \times n_S n_E}$ and the vector $\vec{g}_l$ gives the second derivative of the single measurements $\vec{g}_k$ with the central difference. On the left-hand side of the equation the vector is elongated with zeros, hence the optimization algorithm minimizes the second derivative and thus leads to smoother spectra. The degree of regularization can be influenced via the regularization parameter α. Low values of α reduce the influence whereas higher values increase the influence of the second derivative. The same procedure is used to regularize between measurements with the matrix $\boldsymbol{C} \in \mathbb{R}^{(n_E-2)n_S \times n_E n_S}$ and the according regularization parameter γ. To calculate the derivatives, the matrices are defined as

$$\begin{aligned} \boldsymbol{D} &= \left(D_{ij}\right) = \left(\delta_{ij} - 2\delta_{i(j-1)} + \delta_{i(j-2)}\right) \\ \boldsymbol{C} &= \left(C_{ij}\right) = \left(\delta_{ij} - 2\delta_{i(j-nS)} + \delta_{i(j-2nS)}\right) \end{aligned}$$

using the Kronecker δ_{ij} to achieve a compact notation.

Instead of calculating the spectrum it is possible to calculate the cumulative sum $\vec{G}_l \in \mathbb{R}^{n_S n_E}$ of the spectrum. Therefore, an additional matrix $\boldsymbol{T} \in \mathbb{R}^{n_S \times n_S}$ is introduced:

$$\boldsymbol{T} = \left(T_{ij}\right) = \delta_{ij} - \delta_{(i-1)j}$$

which leads to

$$\vec{g} = \boldsymbol{T} \cdot \vec{G} \,.$$

and hence it is

$$\vec{d} = \begin{pmatrix} \hat{\vec{y}}_l^T & \vec{0}^T & \vec{0}^T \end{pmatrix}^T = \underbrace{\begin{pmatrix} \left(\hat{\boldsymbol{A}}_{\boldsymbol{l}} \cdot (\boldsymbol{I}_{\boldsymbol{l}} \otimes \boldsymbol{T})\right)^T & \alpha \boldsymbol{D}^T & \gamma \boldsymbol{C}^T \end{pmatrix}^T}_{\boldsymbol{M}} \cdot \vec{G}_l + \begin{pmatrix} \hat{\vec{r}}_l^T & \vec{0}^T & \vec{0}^T \end{pmatrix}^T .$$

DOI: 10.1002/mrc.4836

Using this method the regularization is applied to the cumulative sum of the spectra.

Fig. 1 shows the cumulative sum of an exemplary spectrum. The black arrows indicate the direction of the regularization. Typically, only the matrix $\boldsymbol{D}$ is used to regularize in the direction of decay times. The newly introduced matrix $\boldsymbol{C}$ regularizes additionally in the direction of the measurements. Finally, this linear least-squares problem is solved using MATLAB with the objective function (OF):

$$OF = \min_{\vec{G}_l} \frac{1}{2} \left|\left| \boldsymbol{M} \cdot \vec{G}_l - \vec{d} \right|\right|_2^2 \quad \text{such that} \quad \begin{cases} \boldsymbol{T_l} \cdot \vec{G}_l & \geq & \vec{0}, \\ \boldsymbol{F_l} \cdot \vec{G}_l & = & \vec{0}. \end{cases},$$

and constraints to incorporate a priori knowledge into the solution. For instance the cumulative sum has to increase monotonically and hence the first derivative ($\boldsymbol{T} \cdot \vec{G}$) of the cumulative sum has to be greater than zero. Also, the first point of the cumulative sum ($\boldsymbol{F} \cdot \vec{G}$) must be zero. The first element of the matrix $\boldsymbol{F} \in \mathbb{R}^{n_S \times n_S}$ is one, all other elements are zero.

2.2 Evaluating experimental or simulated data

To invert the Laplace transformation, a challenging task is to select suitable regularization parameters. Since in most cases the original spectrum is unknown, one way to estimate the

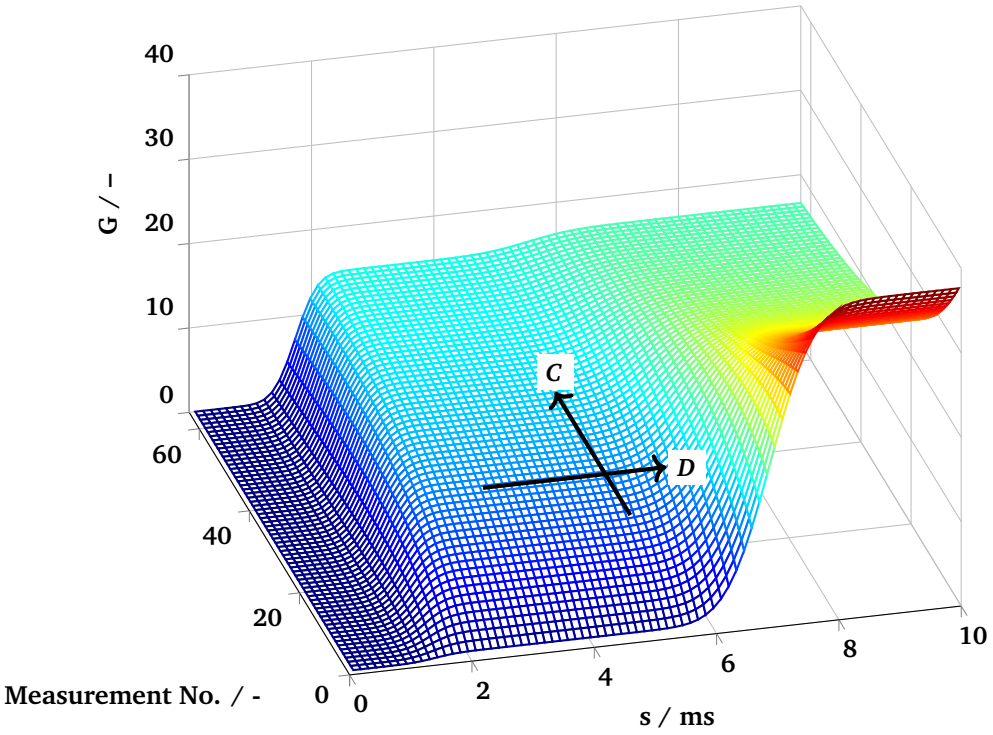

Figure 1: Cumulative sum of the simulated spectrum. The black arrows indicate the direction of the regularization by the matrices $\boldsymbol{C}$ and $\boldsymbol{D}$.

DOI: 10.1002/mrc.4836

regularization parameter is to use the L-Curve method [26]. Therefore, the OF is minimized for 80 different regularization parameters. The cost function

$$\left|\left|\boldsymbol{D}\cdot\vec{G}_l\right|\right|_2^2+\left|\left|\boldsymbol{C}\cdot\vec{G}_l\right|\right|_2^2$$

plotted against the squared norm of residuals

$$\left|\left|\hat{\boldsymbol{A}}_{\boldsymbol{l}}\cdot\vec{g}_l-\hat{\vec{y}}_l\right|\right|_2^2$$

results in an L-shaped curve. Each point of this curve corresponds with a certain combination of regularization parameters α and γ. At the point of maximal curvature, a good trade off between regularization and residuals is obtained. To increase the speed of the L-curve calculation the ratio between α and γ was fixed to $\gamma = 5\alpha$, thus regularizing the second dimension stronger than the first dimension.

3 Experimental

3.1 Generating simulated data

To compare the performance of two-dimensional with conventional regularization, simulated measurement data is generated. The simulated spectrum is calculated with the function:

$$\begin{aligned}\left(g_{l,s}\right) =& a1\exp\left(-3\frac{l}{n_E}\right)\exp\left(-\frac{\left(s-\mu_1\left(1-0.2\frac{l}{n_E}\right)\right)^2}{\sigma_1^2}\right)+\\ & a2\left(1-\exp\left(-3\frac{l}{n_E}\right)\right)\exp\left(-\frac{\left(s-\mu_2\left(1+0.2\frac{l}{n_E}\right)\right)^2}{\sigma_2^2}\right)\end{aligned}$$

and the parameters:

$a1$	0.8	$a2$	0.65
μ_1	7.0	μ_2	1.5
σ_1	0.8	σ_2	0.4
n_S	331	n_E	64

resulting in a spectrum with one ascending and one descending peak in the series dimension. The spectrum is calculated for $n_S = 331$ decay times linearly distributed from 0.2 ms to 10.0 ms and $nE = 64$ measurements. The ideal digitized measurement signal is calculated with

$$\vec{y}_{l,\text{simulated}} = \boldsymbol{A}_{\boldsymbol{l}}\cdot\vec{g}_{l,\text{simulated}}$$

DOI: 10.1002/mrc.4836

for 250 digitized times ranging from 0.02 ms to 20 ms. 5 % white noise is added to the ideal measurement signal, resulting in a signal to noise ratio (SNR) from 13.1 dB to 18.7 dB across the different spectra.

For the Laplace inversion the vector $\vec{s}$ holds 80 digitized decay times ranging from 0.1 ms to 10 ms. Because this vector contains less decay times than the original noise-free vector, the intensity of the weights $\vec{g}$ differ. Therefore, the simulated spectrum is also calculated for the shorter vector $\vec{s}$ and the weights are adjusted accordingly, so it can be compared to those obtained by the Laplace inversion. Fig. 2 shows the simulated measurement signal and the simulated spectrum obtained with this method.

3.2 Furfuryl alcohol polymerization

Vargas et al. analyzed the transverse NMR relaxation of Furfuryl alcohol polymerization in situ. The NMR data was kindly provided by Prof. Guthausen[1][20]. To perform the measurements the "Bruker the minispec" device is used. A total of 64 scans with 5000 echoes and 0.025 ms echo time are conducted per in situ measurement with a home-built NMR-device with a ^{1}H Larmor-frequency of 23 MHz and a measurement depth of 2 mm. Since the polymerization and curing of resins is usually done in sheets, a single-sided NMR device is used for the acquisition. The detailed measurement setup is described in [20]. The data is fitted using a bi-exponential model to calculate the curing degree with the obtained decay times using the dependence of transverse magnetization relaxation on crosslink density.

3.3 Cement hydration

The hydration of ordinary portland cement (CEM I 42.5 R-NA/LA according to DIN EN 197-1) was investigated with a Bruker minispec mq10 low field NMR analyzer with custom-built probe head. The used cement paste has a water to cement ratio of 0.4 and is mixed before filling it into a sample tube with 10 mm diameter. The sample height of 20 mm fits into the entire field of view of the NMR device. Moisture exchange is prevented by sealing the sample tube. The ambient temperature in the measurement chamber is set to 35 °C. CPMG echos are recorded during acquisition. To improve the signal-to-noise ratio 400 scans per time step are averaged. For each in situ hydration experiment 158 measurements at hydration times ranging from 0 h to 60 h were evaluated. Thus, the series dimension n_E contains 158 single measurements.

[1]Institute of Mechanical Process Engineering and Mechanics, KIT, Germany

DOI: 10.1002/mrc.4836

4 Results and discussion

4.1 Simulated data

The simulated measurement signal prepared as described in Sec. 3.1 with 5 % white noise was used for the Laplace inversion. The inversion was performed with the second derivative regularization in the conventional way and with the newly introduced two-dimensional regularization in the series dimension.

Fig. 2 shows the results for the Laplace inversion. Four exemplary simulated measurement signals with noise are depicted on the top left. On the top right the original spectrum, which is the ideal solution to the Laplace inversion is shown. On the middle left the calculated spectrum is shown for the one-dimensional Laplace inversion with a regularization parameter of $\alpha = 4.86$ determined by the L-curve method [4]. The two peaks of the original spectrum can be seen, however they are much broader and hence the intensity is lower. On the middle right, the result of the two-dimensional regularization is shown with the regularization parameters $\alpha = 0.1495$ and $\gamma = 0.7425$. As can be seen, with the additional regularization the spectra are in good agreement to the original spectra. The peaks are narrower and especially the second peak is clearer. The first drop of the second peak is not reproduced for the first 15 spectra and in the last spectra the second peak disappears completely. However, using the regularization in the series dimension, peaks in the spectra can be separated whereas the conventional Laplace inversion would yield one broad peak. With the Frobenius norm the performance of the Laplace inversion is determined quantitatively. Therefore, the Frobenius norm

$$\left|\left|\boldsymbol{g}_{\text{simulated}} - \boldsymbol{g}_{\text{calculated}}\right|\right|_F$$

was calculated using the matrices $\boldsymbol{g} \in \mathbb{R}^{n_S \times n_E}$ holding the entire spectra for a measurement series. Using the one-dimensional Laplace regularization with the L-curve determined regularization parameter $\alpha = 4.86$ from Fig. 2 middle left, the Frobenius norm equals 33.54. When using the same regularization parameter as for the two-dimensional regularization, but with the regularization in the second dimension switched off ($\alpha = 0.1495$, $\gamma = 0$), the Frobenius norm equals to 37.35. In the case of two-dimensional regularization with $\alpha = 0.1495$ and $\gamma = 0.7425$ (Fig. 2 middle right), the Frobenius norm is 17.86 and thus much lower than in the other two cases. This indicates that the two-dimensional regularization is able to reproduce the original spectra much better than the one-dimensional regularization.

On the bottom of Fig. 2 the integrals of the spectra are shown. On the left the integral of the spectrum with the one-dimensional regularization and a large value of α and on the right the integral of the spectra obtained by two-dimensional regularization are shown. With the two-dimensional regularization the integral of the spectrum is much closer to the original spectrum.

To investigate the complexity class of the algorithm, the runtime of the program was measured by inverting a repeated simulated signal with n_E values ranging from 1 to 10 000. The calculations were performed on a standard PC with 16 GB RAM on a single CPU core. For up

DOI: 10.1002/mrc.4836

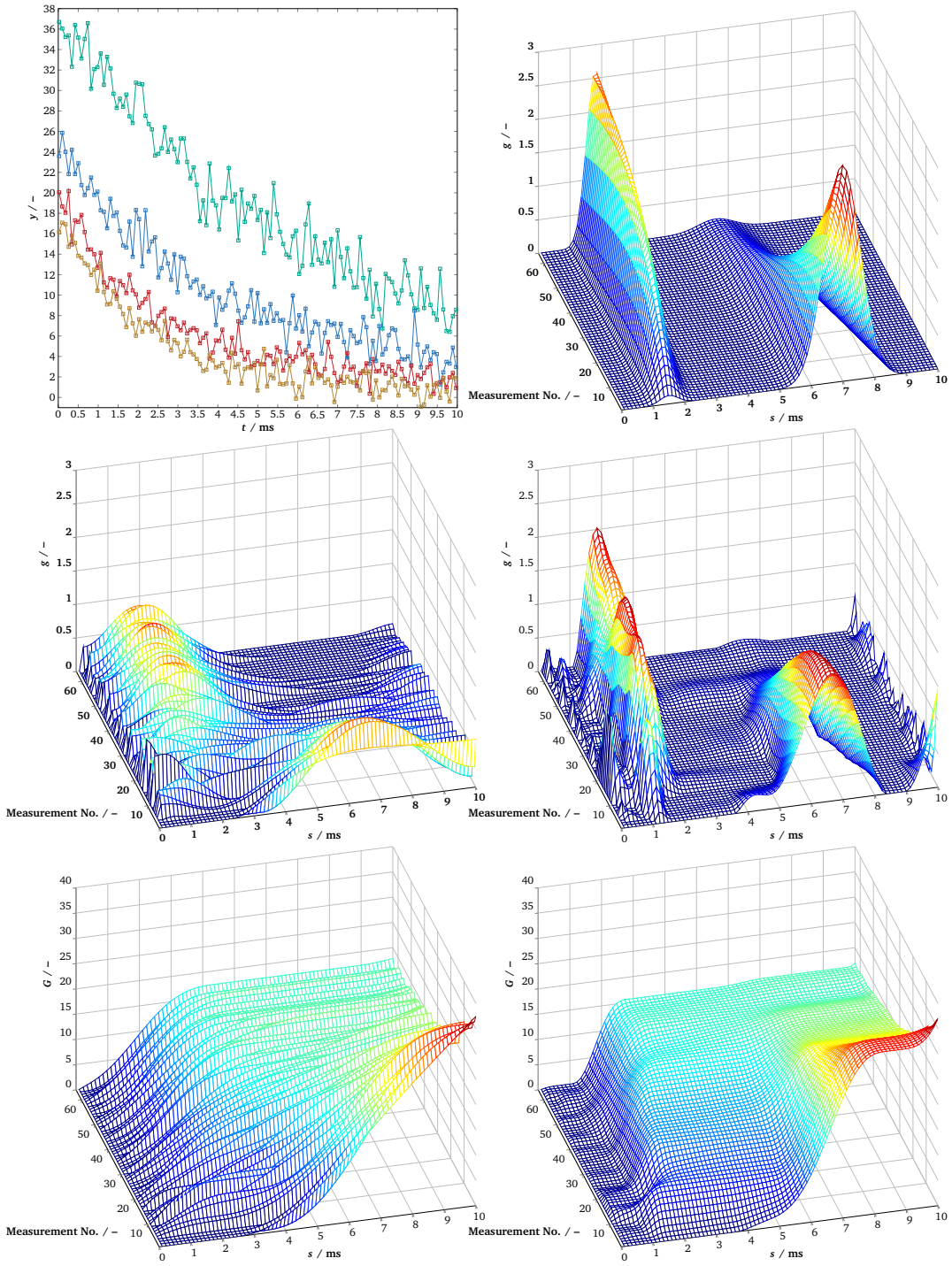

Figure 2: Top left: simulated measurement signal with noise; Top right: simulated spectrum; Middle left: spectrum obtained with one-dimensional Laplace inversion of the simulated signal; Middle right: spectrum obtained with two-dimensional Laplace inversion of the simulated signal. Bottom left: integral of the spectrum obtained by one-dimensional Laplace inversion; Bottom right: integral of spectrum obtained by two-dimensional Laplace inversion.

DOI: 10.1002/mrc.4836

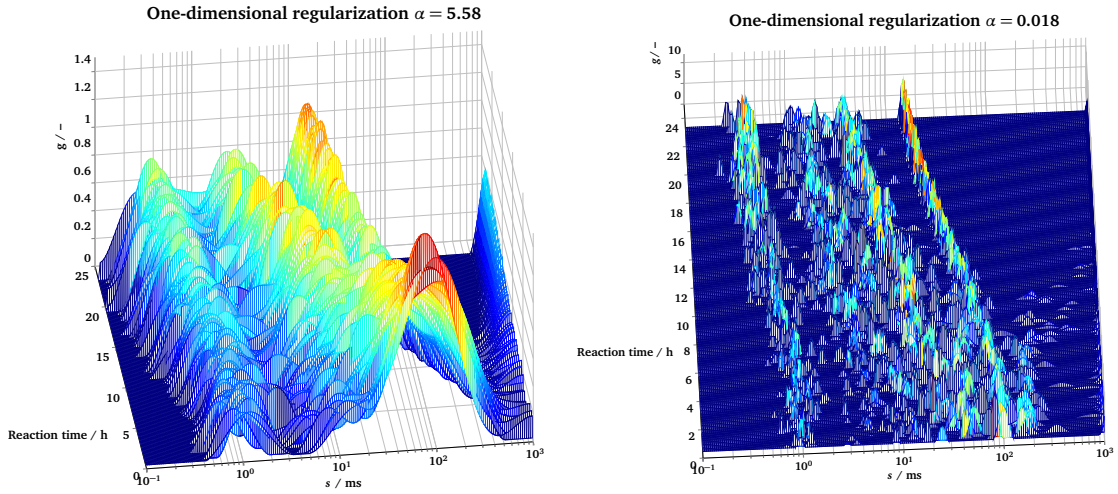

Figure 3: Left: Spectra of Furfuryl alcohol polymerization obtained with one-dimensional regularization and regularization parameter obtained with the L-curve method. Right: Spectra for the same sample using a lower regularization parameter.

to 1000 elements in the series dimension the calculations take less than one minute. The measured runtimes indicate a polynomial runtime behaviour $\mathcal{O}\left(n^k\right)$.

4.2 Furfuryl alcohol polymerization

To monitor Furfuryl alcohol polymerization reaction in situ NMR measurements were conducted as described in Sec. 3.2. The conventional one-dimensional Laplace inversion spectra are depicted in Fig. 3. On the left side, the regularization parameter of $\alpha = 5.58$ was chosen using the L-curve method. The resulting spectra show two main peaks at the very beginning, which then separate into three peaks with increasing reaction time. The peaks are broad and shift towards smaller decay times with increasing reaction time. Selecting a suitable regularization parameter is often a challenging task. The L-curve method provides an instrument to estimate such a regularization parameter, but then often leads to quite broad peaks. On the right-hand side of Fig. 3, a lower regularization parameter of $\alpha = 0.018$ is used. As can be seen, two main peaks form with a third peak scattering between the two main peaks. The total spectrum however is not as clear because the position and width of peaks shift between the single spectra. Also, several additional peaks between the main features appear and disappear which makes the interpretation of such spectra a difficult task.

Fig. 4 shows spectra obtained with the proposed two-dimensional regularization procedure for the Furfuryl alcohol polymerization data set. With the determined regularization parameters of $\alpha = 0.018$ and $\gamma = 0.090$, four peaks appear in the spectrum. Those peaks are separated clearly and are narrower than the peaks obtained with the regular Laplace inversion method. All four peaks shift towards smaller decay times with increasing reaction time. The peaks at

DOI: 10.1002/mrc.4836

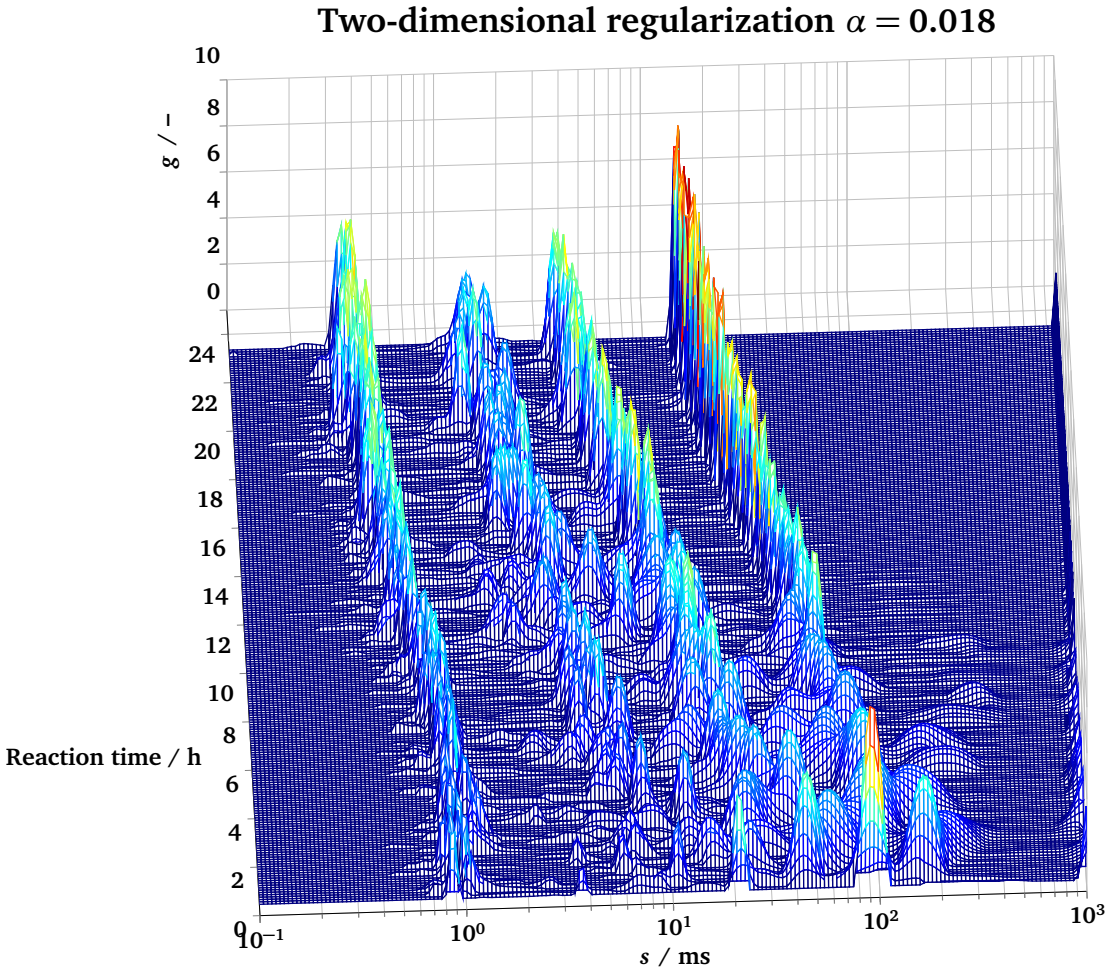

Figure 4: Two-dimensional regularization for the Furfuryl alcohol polymerization.

the smallest and highest obtained decay times also increase in intensity whereas the intensity of the two middle peaks does not change significantly after the first hours. A significant improvement by the two-dimensional regularization can be observed when comparing the spectra of Fig. 3 right with Fig. 4. In both cases the same value for the regularization parameter α is used, but only with the two-dimensional regularization features of the spectra can be separated. Hence, the regularization in the second dimension allows to reduce the regularization parameter for the first dimension. The treatment of the measurement series as one object does by itself not improve the regularization result. In Fig. 3 right the regularization parameter for the second dimension is $\gamma = 0$ but the inversion algorithm is the same. Setting $\gamma = 0$ yields the same results as the separate treatment of each single spectrum. The improvement of the regularization in the second dimension can be seen clearly in Fig. 4. When comparing to Fig. 3 left, where the regularization parameter of $\alpha = 5.58$ was chosen with the L-curve method, the peaks are now much narrower and the features better

DOI: 10.1002/mrc.4836

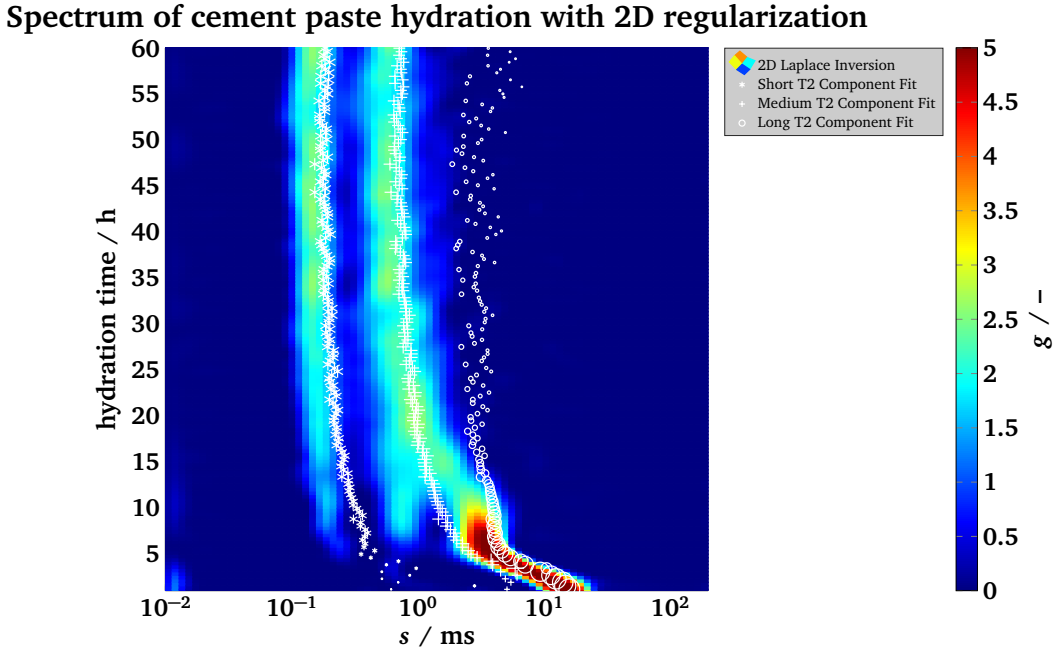

Figure 5: Two-dimensional Laplace inversion of T_2 decay on a hydrating cement sample. The white symbols show the calculated tri-exponential fit for the NMR measurement data.

separated.

Vargas et al. used a bi-exponential fit to obtain the T_2 decay times from the measurement data [20]. Exponential fitting is a method often used for the analysis of NMR relaxation data. The spectra obtained by the Laplace inversion indicate that a tri-exponential or quad-exponential fit might be more suitable for the measurement data, especially at higher reaction times. However, whereas tri-exponential fitting is often possible, quad-exponential fitting is numerically difficult.

4.3 Cement hydration

The results from hydration measurements with portland cement paste are displayed in Fig. 5. The intensity of the Laplace inverted spectrum is shown by color coding. The two-dimensional Laplace inversion regularization parameters $\alpha = 0.015$ and $\gamma = 0.075$ were determined with the L-curve method. The white markers show the results of a tri-exponential fit. Marker sizes are scaled according to the intensity of the respective relaxation component. Right after mixing the cement paste a single characteristic relaxation component close to 10 ms can be detected with both analysis methods. During the following hours a shift of the decay time towards smaller decay times can be observed for up to 5 hours hydration time. This can be explained by the formation of nano-scale Calcium-Silicate-Hydrate phases and the successive

DOI: 10.1002/mrc.4836

chemical and physical binding of water. For this region a mono-exponential fit may be utilized as well. Starting at about 5 hours hydration time hydration products with significantly lower relaxation times evolve whereas intensity of the initially observed component decreases. The tri-exponential fit is unable to reflect peak broadening as seen with the Laplace inversion. For long hydration times, two relaxation components are formed and the tri-exponential fit shows low intensity and high scatter for the longest relaxation component. Both Laplace inversion with series regularization and tri-exponential fit show similar relaxation components and intensities. In the case of hydration studies the Laplace inversion leads to refined spectral information and offers additional information on the spectral shape of T_2 decay components. Regularization in the second dimension, e. g. hydration time, can further reduce the number of repetition measurements applied to improve signal-to-noise ratio by using a priori knowledge of the spectral evolution in the hydration time domain.

5 Conclusions

The main requirement for the use of two-dimensional regularization is a steady and continuous evolution of the spectra in the second dimension. This is true for reaction kinetics, adsorption and desorption or diffusion processes. The second dimension does not have to be a time scale. Basically, any series of measurements with a continuous and steady development in second dimension are suitable for the proposed Laplace inversion method. For other cases with erratic changes between single measurements the two-dimensional regularization is not an appropriate data analysis technique.

Finding a good set of regularization parameters is still a challenging task. With the additional regularization in the second dimension, the amount of regularization in the first dimension can be reduced and hence seperate peaks, which could not be resolved otherwise. Using the L-curve method allows to estimate suitable regularization parameters. The disadvantage of the L-curve method is the requirement to perform the entire Laplace inversion for multiple regularization parameters to actually get the L-curve. Depending on the dataset size this can be a time-consuming task. For large series, processing times of several hours can be required to calculate the L-curve on personal computers, so that e. g. implementations without Kronecker product could be beneficial.

The Laplace inversion with two-dimensional regularization presented in this study shows a significant improvement compared to the one-dimensional regularization method. This could be shown for simulated data and also for the two practical use cases Furfuryl alcohol polymerization and hydrating cement paste kinetics. The two-dimensional regularization allows a more generic approach for the analysis of NMR data than exponential fitting and yields to more conclusive spectra than the Laplace inversion with one-dimensional regularization. This method is hence a helpful tool, especially for noisy measurement data with multiple decay components. Further applications investigating the benefit of regularization in series dimension would be welcome, the corresponding author can provide the used implementation.

DOI: 10.1002/mrc.4836

References

[1] B. Blumich, *Essential NMR*. Berlin, Heidelberg: Springer-Verlag Berlin Heidelberg, 2005.

[2] E. H. Hardy, *NMR Methods for the Investigation of Structure and Transport*. Berlin, Heidelberg: Springer-Verlag Berlin Heidelberg, 2012.

[3] S. W. Provencher, "CONTIN: A general purpose constrained regularization program for inverting noisy linear algebraic and integral equations", *Comput. Phys. Commun.*, vol. 27, no. 3, pp. 229–242, 1982.

[4] P. C. Hansen, "Analysis of discrete ill-posed problems by means of the L-curve", *SIAM Rev.*, vol. 34, no. 4, pp. 561–580, 1992.

[5] I. J. Day, "On the inversion of diffusion nmr data: Tikhonov regularization and optimal choice of the regularization parameter.", *J. Magn. Reson.*, vol. 211, pp. 178–185, 2 2011.

[6] M. A. Delsuc and T. E. Malliavin, "Maximum entropy processing of DOSY NMR spectra", *Anal. Chem.*, vol. 70, no. 10, pp. 2146–2148, 1998.

[7] A. Cherni, E. Chouzenoux, and M.-A. Delsuc, "PALMA, an improved algorithm for DOSY signal processing", *Analyst*, vol. 142, no. 5, pp. 772–779, 2017.

[8] M. Urbańczyk, D. Bernin, W. Koźmiński, and K. Kazimierczuk, "Iterative thresholding algorithm for multiexponential decay applied to PGSE NMR data", *Anal. Chem.*, vol. 85, no. 3, pp. 1828–1833, 2013.

[9] K. Xu and S. Zhang, "Trust-region algorithm for the inversion of molecular diffusion NMR data", *Anal. Chem.*, vol. 86, no. 1, pp. 592–599, 2014.

[10] G. C. Borgia, R. J. S. Brown, and P. Fantazzini, "Uniform-penalty inversion of multiexponential decay data", *J. Magn. Reson.*, vol. 132, no. 1, pp. 65–77, 1998.

[11] Y.-Q. Song, L. Venkataramanan, M. D. Hürlimann, M. Flaum, P. Frulla, and C. Straley, "T(1)–T(2) correlation spectra obtained using a fast two-dimensional Laplace inversion", *J. Magn. Reson.*, vol. 154, no. 2, pp. 261–268, 2002.

[12] M. D. Hürlimann and L. Venkataramanan, "Quantitative measurement of two-dimensional distribution functions of diffusion and relaxation in grossly inhomogeneous fields", *J. Magn. Reson.*, vol. 157, no. 1, pp. 31–42, 2002.

[13] L. Venkataramanan, Y.-Q. Song, and M. D. Hürlimann, "Solving Fredholm integrals of the first kind with tensor product structure in 2 and 2.5 dimensions", *IEEE Trans. Signal Process.*, vol. 50, no. 5, pp. 1017–1026, 2002.

[14] Y.-Q. Song, L. Venkataramanan, and L. Burcaw, "Determining the resolution of Laplace inversion spectrum", *J. Chem. Phys.*, vol. 122, no. 10, p. 104 104, 2005.

[15] V. Bortolotti, R. J. S. Brown, P. Fantazzini, G. Landi, and F. Zama, "Uniform Penalty inversion of two-dimensional NMR relaxation data", *Inverse Prob.*, vol. 33, no. 1, 2017.

DOI: 10.1002/mrc.4836

[16] S. Campisi-Pinto, O. Levi, D. Benson, M. Cohen, M. T. Resende, M. Saunders, C. Linder, and Z. Wiesman, "Analysis of the Regularization Parameters of Primal-Dual Interior Method for Convex Objectives Applied to H-1 Low Field Nuclear Magnetic Resonance Data Processing", *Appl. Magn. Reson.*, vol. 49, no. 10, 1129–1150, 2018.

[17] X. Ge, H. Wang, Y. Fan, Y. Cao, H. Chen, and R. Huang, "Joint inversion of T-1 -T-2 spectrum combining the iterative truncated singular value decomposition and the parallel particle swarm optimization algorithms", *Comput. Phys. Commun.*, vol. 198, 59–70, 2016.

[18] S. Huber, A. Haase, and B. Gleich, "Analysis of 2D NMR relaxation data using Chisholm approximations", *J. Magn. Reson.*, vol. 281, 66–74, 2017.

[19] D. Medellin, V. R. Ravi, and C. Torres-Verdin, "Multidimensional NMR inversion without Kronecker products: Multilinear inversion", *J. Magn. Reson.*, vol. 269, 24–35, 2016.

[20] M. A. Vargas, M. Scheubner, and G. Guthausen, "Reaction kinetics of polyfurfuryl alcohol bioresin and nanoparticles by 1 H-NMR transverse relaxation measurements", *Polym. Compos.*, vol. 39, no. 9, pp. 3280–3288, 2017.

[21] J. Greener, H. Peemoeller, C. Choi, R. Holly, E. J. Reardon, C. M. Hansson, and M. M. Pintar, "Monitoring of hydration of white cement paste with proton nmr spin–spin relaxation", *J. Am. Ceram. Soc.*, vol. 83, no. 3, pp. 623–627, 2000.

[22] J. Mitchell, J. B. W. Webber, and J. H. Strange, "Nuclear magnetic resonance cryoporometry", *Phys. Rep.*, vol. 461, no. 1, pp. 1–36, 2008.

[23] O. V. Petrov and S. Stapf, "Parameterization of NMR relaxation curves in terms of logarithmic moments of the relaxation time distribution", *J. Magn. Reson.*, vol. 279, 29–38, 2017.

[24] P. Stilbs, "Fourier transform pulsed-gradient spin-echo studies of molecular diffusion", *Prog. Nucl. Magn. Reson. Spectrosc.*, vol. 19, no. 1, pp. 1–45, 1987.

[25] B. Yuan, Y. Ding, G. M. Kamal, L. Shao, Z. Zhou, B. Jiang, P. Sun, X. Zhang, and M. Liu, "Reconstructing diffusion ordered NMR spectroscopy by simultaneous inversion of laplace transform", *J. Magn. Reson.*, vol. 278, pp. 1–7, 2017.

[26] P. C. Hansen, "The L-curve and its use in the numerical treatment of inverse problems", in *Computational inverse problems in electrocardiography*, ser. Advances in Computational Bioengineering Series, P. Johnston, Ed., Southampton: WIT Press, 2001, pp. 119–142.

Acknowledgments

The authors thank the German Research Foundation for funding the projects MU 1368/13-1 and HA 2840/6-1. G. Guthausen, Karlsruher Institut of Technology, G. Gross and K. Zick, Bruker Corporation, J. Sester and V. Spinnler are acknowledged for providing experimental data and helpful discussion.

DOI: 10.1002/mrc.4836

Published article

This is the accepted version of the following article: B. Radel *et al.*, "Regularized inversion of the laplace transform for series of experiments", *Magn. Reson. Chem.*, vol. 57, pp. 836–844, 10 2019, which has been published in final form at `https://dx.doi.org/10.1002/mrc.4836`. This article may be used for non-commercial purposes in accordance with the Wiley Self-Archiving Policy [http://www.wileyauthors.com/self-archiving].

DOI: `10.1002/mrc.4836`